NATIONAL ADVISORY COMMITTEE FOR AERONAUTICS

TECHNICAL NOTE 2711

THE AERODYNAMIC DESIGN OF HIGH MACH NUMBER NOZZLES UTILIZING AXISYMMETRIC FLOW WITH APPLICATION TO A NOZZLE OF SQUARE TEST SECTION

By Ivan E. Beckwith, Herbert W. Ridyard, and Nancy Cromer

Langley Aeronautical Laboratory
Langley Field, Va.

Washington

June 1952

1E

NATIONAL ADVISORY COMMITTEE FOR AERONAUTICS

TECHNICAL NOTE 2711

THE AERODYNAMIC DESIGN OF HIGH MACH NUMBER NOZZLES UTILIZING AXISYMMETRIC FLOW WITH APPLICATION TO A NOZZLE OF SQUARE TEST SECTION

By Ivan E. Beckwith, Herbert W. Ridyard, and Nancy Cromer

SUMMARY

A method is given for the design of three-dimensional nozzles utilizing axisymmetric flow. The nozzle can be designed to produce uniform flow in a test chamber of arbitrary cross section. The method is applied to obtain the final coordinates of a Mach number 10 nozzle for which a square test section is specified to reduce the possibility of axisymmetric imperfections at the wall and to provide for the installation of schlieren windows. Radial flow is used in a portion of the flow field to reduce the computation time. The remainder of the flow field is computed by the method of characteristics, but a simplified method is used near the axis. Tables which facilitate computation of the radial flow and the flow near the axis are included. Transition streamlines determined from the analytic expressions of Kuno Foelsch are compared with the streamlines obtained from the characteristics net of the Mach number 10 nozzle. The Foelsch streamlines deviate from the flow-net streamlines by as much as 12 percent. Similar analytic expressions are derived from the geometric properties of the flow. These new expressions result in transition streamlines with a maximum error of about 4 percent.

INTRODUCTION

Recent research has indicated that three-dimensional supersonic nozzles may become more desirable for high Mach number tunnels than conventional two-dimensional nozzles. For example, in two-dimensional nozzles designed for test Mach numbers much greater than 5, the flow is very sensitive to any change of the extremely small dimensions at the minimum section. The high temperatures required to avoid liquefaction of the air at these high Mach numbers make the problem of obtaining dimensional stability of the small slit-like minimum extremely difficult. (See reference 1.) In addition, the excess growth of boundary layer along the center of the nozzle side plates may also interfere with the

design flow. A two-stage nozzle discussed in reference 2 avoids the first difficulty but fails to operate satisfactorily primarily because of the excess boundary layer. Consideration of three-dimensional nozzles thus becomes imperative not only for tests of stationary models at the higher Mach numbers but also for ballistic tests where the projectile must pass through the minimum of a supersonic nozzle.

A method for the design of three-dimensional nozzles based on axisymmetric flow is presented in this paper. Although the flow is axisymmetric throughout, the final cross-sectional shape of the nozzle may be arbitrary. The general concept for the determination of the arbitrary cross-sectional shape was applied to the design of an axisymmetric nozzle at the Langley Aeronautical Laboratory by Mr. Morton Cooper in 1947. The design method presented in this paper is general; however, as an illustrative example the design of a Mach number 10 nozzle with a square test section is included. Specification of a square cross-sectional shape for the test chamber provides for the installation of conventional schlieren windows. A further advantage of the resulting noncircular walls is that the possibility of incurring axisymmetric imperfections at the nozzle wall is reduced. Disturbances originating from axisymmetric imperfections focus along the axis of the nozzle. This focusing effect has been known to cause disturbances of considerable magnitude in the vicinity of the nozzle axis. A theoretical analysis of the three-dimensional focusing effect is given in reference 3, part II.

LIST OF SYMBOLS

A, A', B, C, D, E, P, K	points in axisymmetric flow field as indicated in figure 1 or sketch on p. 10; used as subscripts for conditions at these points
c	local speed of sound
M	Mach number
V	velocity (with bar to indicate vector quantity)
r	distance measured from source point in radial flow field
r_{cr}	distance measured from the source point to sonic sphere in radial flow
x, R, ϕ	cylindrical coordinates for flow field and nozzle
s	distance along a Mach line measured in meridian plane from the axis of symmetry

x,y,z	Cartesian coordinates for nozzle
μ	Mach angle, $\sin^{-1} 1/M$
γ	ratio of specific heats = 1.400 throughout
θ	local flow angle
θ_I	total expansion angle integrated from the sonic line in meridian plane
ρ	density
ψ	stream function for a compressible axisymmetric flow
$\overline{\psi}$	dimensionless stream function

Subscripts:

r	radial flow
o	isentropic deceleration to zero velocity

NOZZLE DESIGN

For convenience in discussion, the nozzle is divided into four regions: I, approach; II, throat; III, radial flow; and IV, transition region, as indicated in figure 1.

Approach.- The specification of parallel flow at the minimum section facilitates the computation of the supersonic portion of the flow. Theoretical methods (references 4 and 5) are available for the design of an approach to give parallel flow; however, it is usually more conservative to base the approach-section design on existing wind tunnels which have the desired characteristics. The coordinates for the approach of the Mach number 10 nozzle were therefore adapted from those used in the Langley 8-foot high-speed tunnel. In the absence of a better criterion the square approach section was obtained by using the same rate of area change with axial distance as in the circular approach of the Langley 8-foot high-speed tunnel.

Radial flow.- Construction of the supersonic flow field may start with either an arbitrary streamline A'C (fig. 1) together with an assumed flow distribution in the minimum or with the specification of a flow distribution along the axis of symmetry of the flow. The second specification was chosen in this investigation primarily to expedite the computation procedure; however, if this center-line distribution were

entirely arbitrary, the extent of a physically possible flow would be severely limited; that is, Mach lines of the same family would converge too rapidly or intersect before the computation had proceeded far enough from the axis to result in a well-proportioned nozzle. This difficulty is avoided by specifying radial flow along a portion of the axis such as line BD. If this specification is used, the flow can be immediately determined for region III from the radial-flow equations and, in general, a physically possible flow results for region II.

The use of radial flow in a part of the flow field has the additional advantage of reducing the computing time, since the flow properties along the bounding Mach lines BC and CD can be determined exactly without recourse to the step-by-step method of characteristics. The equations for three-dimensional radial flow are based on the assumption of spherical symmetry. The resulting simplification of the general equations of motion allows their integration in closed form as indicated in reference 6 and 7. In addition, it is possible to integrate the characteristic equations as in two-dimensional steady isentropic flow. For convenience, the three-dimensional radial-flow equations based on the general steady-flow relations (for example, reference 8) are presented in the Appendix. Values have been calculated by use of these radial-flow equations and the results are tabulated for a range of parameters from $M = 1.0$ to $M = 11.93$ in table I. This change in M corresponds to a change in expansion angle θ_I, which is used as the argument, from 0° to 53.375°.

If point C is at the intersection of the Mach lines bounding the radial-flow region, as illustrated in figure 1, it will be the inflection point on the streamline A'CE. This streamline may be taken as the wall of a nozzle, and the maximum wall angle and the coordinates of the inflection point can then be determined immediately from the local flow angle at C. The value of the flow angle at C is entirely arbitrary; however, a reasonable value can be determined as a compromise between the requirements for over-all nozzle length and maximum rate of expansion. For the Mach number 10 nozzle, the flow angle at C was taken as 16°.

Throat.- The flow in region II (the throat) is computed by the method of characteristics with the initial conditions of a known flow distribution along line BC from radial flow and an arbitrary distribution along line AB as shown in figure 1. The Mach number 10 nozzle computation was simplified by taking the arbitrary distribution as a straight line with a slope given by the radial flow at point B. In general, this assumption is incompatible with a straight sonic line; indeed, a necessary condition for a straight sonic line is $\left(\frac{\partial M}{\partial x}\right)_{M=1} = 0$. However, for high Mach number nozzles, this simplifying assumption results in a satisfactory solution because of the small dimensions of the minimum section. The characteristics net for region II is shown in figure 2 with a streamline through point C included.

The characteristic equations may be used in a form where the more usual velocity parameter, such as that used in reference 9, is replaced by the Mach number by using the differential relation between Mach number and velocity. Sample calculations indicate that the use of this parameter for the high Mach number range reduces the numerical error inherent in the method of characteristics. The particular parameter used makes little difference at the lower Mach numbers.

When the Mach number is used as a parameter, the characteristic equations are

$$d\theta \mp \frac{\sqrt{M^2 - 1}}{M\left(1 + \frac{\gamma - 1}{2} M^2\right)} dM \pm \frac{1}{R\left(\sqrt{M^2 - 1} \cot \theta \mp 1\right)} dx = 0 \qquad (1)$$

and

$$dR = \tan(\theta \pm \mu)\, dx \qquad (2)$$

where the upper signs correspond to the left Mach lines and the lower signs to the right Mach lines. The distinction between these Mach lines is illustrated in figure 2. The last term on the left-hand side of equation (1) becomes indeterminate at the axis of symmetry, that is, as R and θ approach zero. If the limit of this term is taken (reference 9) as $R \to 0$, equation (1) becomes

$$d\theta \mp \frac{\sqrt{M^2 - 1}}{M\left(1 + \frac{\gamma - 1}{2} M^2\right)} dM \pm \frac{1}{2} \frac{\sqrt{M^2 - 1}}{M\left(1 + \frac{\gamma - 1}{2} M^2\right)} \left(\frac{\partial M}{\partial x}\right)_{R=0} dx = 0 \qquad (3)$$

Thus, if $\left(\frac{\partial M}{\partial x}\right)_{R=0}$ is specified along the center line, equation (3) may be used in conjunction with equations (1) and (2) to compute the flow.

An alternative method of computing the flow in the vicinity of the axis can be used. This method consists in reducing equation (3) by dividing this equation by dx and using a relation which follows from the general expression for the total derivative of M with respect to x along a Mach line; that is, $dM/dx = \partial M/\partial x + (\partial M/\partial R)(dR/dx)$. If this total derivative is evaluated at $R = 0$, there results the required relation, $dM/dx = (\partial M/\partial x)_{R=0}$, since in axisymmetric isentropic flow $(\partial M/\partial R)_{R=0} = 0$. (See reference 3, part I.)

Hence the characteristic equations evaluated at the axis become

$$d\theta \mp \frac{1}{2} \frac{\sqrt{M^2 - 1}}{M\left(1 + \frac{\gamma - 1}{2} M^2\right)} dM = 0 \qquad (4)$$

Then equations (2) and (4) are used to compute the flow in the immediate vicinity of the axis; that is, at points 2,1; 3,2; 4,3; . . ., in figure 2. Equation (4) is the differential form of the corresponding equation given by Goldstein as a finite-difference equation (reference 3, part I, page 218).

A simplification is possible since equation (4) is of the same form as the corresponding equation for radial flow. (See Appendix.) Hence, the integral of equation (4) or the corresponding tabulated results (table I) can be used, in effect, to determine the hodograph in the region of the axis for any axisymmetric, isentropic flow. The method should be sufficiently accurate even at a small distance from the axis if $\partial M/\partial R$ is small.

The row of points adjacent to the axis in region II (figure 2) have been computed by both equations (3) and (4) for the Mach number 10 nozzle. The results of this computation are compared in table II. The differences between the two methods are small for all the points and tend to decrease as point 2,1 is approached. The remainder of the flow field in region II was then computed with equations (1) and (2) for both methods at the axis. A relative comparison of the effect of the two methods on the rest of the flow field may then be obtained by comparing corresponding streamlines through the two flow fields. If these streamlines are determined by the flow-angle method (described in a subsequent section entitled "Streamlines") starting from point C, for example, and working toward A', accumulative errors arise which prevent the streamlines from passing through the theoretically exact point A'. In this connection it is noted that the R coordinate of point A' can be determined exactly from the mass-flow requirement at the minimum (assuming parallel flow at M = 1 along a line through A' normal to the axis); whereas the x coordinate of A' depends on the assumption made for the flow distribution along the line AB. Thus, if the streamlines in both cases are started at the fixed initial point C, the error in R/r_{cr} at $x = x_A$ was 0.96 percent for the first method (equations (1), (2), and (3)); whereas for the alternate method (equations (1), (2), and the integral of equation (4)), the error was 1.02 percent of the known radius at $x = x_A$.

Transition.- The flow in region IV (transition region) can be computed by equations (1) and (2) from the initial conditions of a radial distribution along the Mach line CD and parallel and uniform flow along the Mach line DE. The characteristics net for region IV in the Mach number 10 nozzle is shown in figure 3 with a streamline through point C included.

Mesh size.- The axisymmetric flow fields in regions II and IV (fig. 1) were computed for the Mach number 10 nozzle by using the method of finite differences applied to equations (1) to (3). The flow for region II was computed with seven steps along line AB and eight steps along line BC as shown in figure 2; the nearest point to the sonic line had a Mach number of 1.019928. Region IV was computed with 2° steps in θ_I along CD and 10 uniformly spaced steps along DE as shown in figure 3. Three iterations were made for each point according to the procedure of reference 9 so that the parameters were allowed to converge to nearly constant values. Altogether, this computation totaled 74 points and was performed on an electrically operated desk-type computing machine at an average rate of 3 hours per point for a total of approximately 220 hours of computing time. Application of the simplified method (integral of equation (4)) at the axis would reduce the total computing time to about 200 hours. Without the specification of radial flow along BD, 21 more points would have been required, and the total computing time would have been increased to about 290 hours.

When a streamline through this flow net was determined, appreciable errors resulted because of the size of the steps chosen for the computation. For this reason, computations were made with a finer flow net with steps approximately 1/3 the size of those in the coarse net previously described and requiring a total of 573 points. The Bell Telephone Laboratories X-66744 relay computer was used to perform this task. The available Bell computing tapes utilized the characteristic equations in the form given in reference 10 and made only two iterations for each point. The Bell computer performed the computation at a rate of 0.3 hour per point for a total of 172 hours.

Sample computations have demonstrated that the values of the flow parameters will converge in the iteration process more rapidly if equations (1) and (2) and the iteration procedure of reference 9 are used instead of the equations and iteration procedure of reference 10. However, a comparison has been made of the accuracy of the flow nets as determined on the desk computer and the Bell computer. The results of this comparison are given in table III, in which the ordinates of the streamlines determined by the flow-angle method are compared with the theoretically exact values at points C and A'. The errors result from the approximations inherent in the finite-step method employed in computing the flow net and are some function of the size of the steps.

Since the results obtained with the Bell computer were more accurate, in spite of the fewer number of iterations made and the slower convergence of the iteration procedure, the advantage of maintaining a fine net is obvious. For these calculations, the increase in accuracy is of the same order as the decrease in mesh size.

Streamlines.- After the flow field has been computed the streamlines may be obtained either from the local flow angles or from the stream function.

Stokes' stream function ψ (reference 8) for an axisymmetric compressible flow can be defined by the differential relation

$$\frac{d\psi}{ds} = \rho R c \tag{5}$$

where ds is the differential distance along a Mach line in the meridian plane. Introducing a dimensionless stream function $\Psi = \frac{\psi}{r_{cr}^2 \rho_o c_o}$ into equation (5) and integrating from the axis $\left(\frac{s}{r_{cr}} = 0\right)$ to $\frac{s}{r_{cr}}$ gives the value of the stream function at $\frac{s}{r_{cr}}$,

$$\Psi_s = \int_0^{s/r_{cr}} \frac{R}{r_{cr}} \frac{1}{\left(1 + \frac{\gamma - 1}{2} M^2\right)^{(\gamma+1)/2(\gamma-1)}} d\left(\frac{s}{r_{cr}}\right) \tag{6}$$

where the isentropic flow relations for ρ/ρ_o and c/c_o have been used. Within the radial flow region BCD (fig. 1), ψ can be defined by the equation

$$\frac{d\psi}{d\theta} = \rho V r^2 \sin\theta \tag{7}$$

Integrating along the arc and dividing by $r_{cr}^2 \rho_o c_o$ yields

$$\Psi = \left(\frac{2}{\gamma + 1}\right)^{\frac{\gamma+1}{2(\gamma-1)}} (1 - \cos\theta) \tag{8}$$

since ρ, V, and r are constants along the arc of radius r. Now the value of Ψ can be found for a given value of θ along the Mach lines CD or BC from equation (8). Then, since Ψ is constant along a streamline, graphical integration of equation (6) along the Mach lines in region II or IV up to the desired value of Ψ locates the remaining points for this streamline. In practice, the most accurate procedure is to obtain a value of Ψ for each point in the Mach net (that is, intersection points of right and left Mach lines) by integrating equation (6) along the left Mach lines. Any desired value of Ψ and the corresponding x and R coordinates are then easily obtained by linear interpolation between the points. Integration along the left Mach lines is more accurate in region IV than integration along the right lines because of the more gradual change in flow variables along the left lines.

The streamlines may also be obtained from the flow angles by extending the streamlines directly through the R - x plane by a step-by-step iteration procedure. This iteration procedure consists of extending the tangent to a streamline from a known point in the flow, such as a point on the Mach lines BC, CD, or DE, until another Mach line is intersected. As an example, consider the streamline through point E, in figure 3. By linear interpolation between the known values of the flow angle at points 1 and 3, a value (say θ_2) is obtained for this first intersection of the tangent line and the Mach line. The mean of θ_2 and the initial value θ_E is then used as the slope for a new line through the initial point. The intersection of this line with the Mach line 1-3 gives a new flow angle θ_2'. This process is repeated until the change in θ_2 for successive iterations is no longer significant, whereupon the entire procedure is repeated in the adjoining mesh.

The flow-angle method was not used for the final computation of the streamlines of the Mach number 10 nozzle because of the accumulative errors at the end points A' and C. Nevertheless, the flow-angle method was found useful for comparing the effect of mesh size on the accuracy of the flow field. The stream-function method results in streamlines with the exact coordinates at points A', C, and D. Furthermore, this method requires less time than the flow-angle method, especially if several streamlines are required as for a nozzle with a square test section. For the Mach number 10 nozzle small local irregularities in the streamlines were eliminated by integrating curves of $\tan \theta$ plotted against x where θ was obtained from the stream-function method.

Foelsch (reference 7) has given analytic expressions for the coordinates of the transition streamlines in a three-dimensional nozzle.

Foelsch's equations may be derived under somewhat more restrictive assumptions from equations (6) and (8) given in this paper. The points in the flow field are identified in the following sketch:

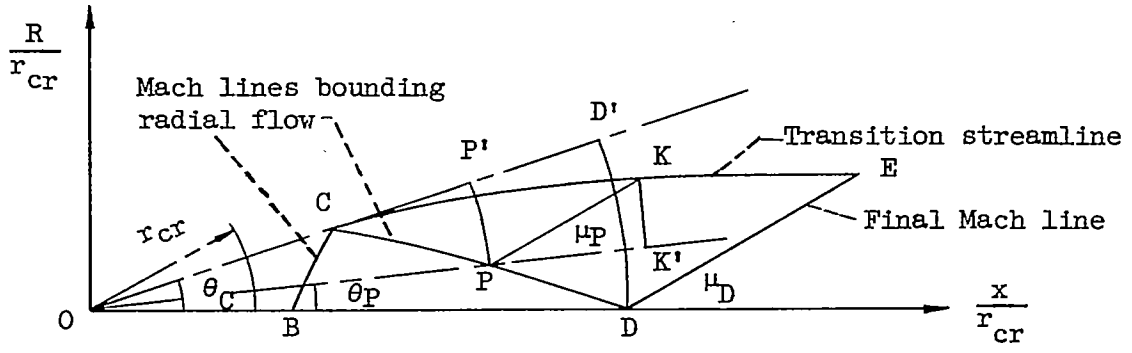

Thus, for any left Mach line PK in the transition region:

$$\Psi_C - \Psi_P = \int_P^K \frac{\frac{R}{r_{cr}}}{\left(1 + \frac{\gamma - 1}{2} M^2\right)^{(\gamma+1)/2(\gamma-1)}} d\left(\frac{s}{r_{cr}}\right) \tag{9}$$

from equation (6). Then, by use of the relation

$$d\left(\frac{s}{r_{cr}}\right) = \frac{d\left(\frac{R}{r_{cr}}\right)}{\sin(\theta + \mu)} = \frac{M\, d\left(\frac{R}{r_{cr}}\right)}{\cos\theta + \sqrt{M^2 - 1}\sin\theta}$$

and equation (8), equation (9) can be written as

$$\cos\theta_P - \cos\theta_C = \int_P^K \frac{M \frac{R}{r_{cr}} d\left(\frac{R}{r_{cr}}\right)}{\left[\frac{2}{\gamma + 1}\left(1 + \frac{\gamma - 1}{2} M^2\right)\right]^{\frac{\gamma+1}{2(\gamma-1)}} \left(\cos\theta + \sqrt{M^2 - 1}\sin\theta\right)} \tag{10}$$

where the integration is along the left Mach line PK. Making the assumption that M and θ are constant along the left Mach lines and equal to their values at P and using the radial flow equations for r_P/r_{cr} and R_P/r_{cr} gives, for equation (10),

$$\frac{R_K}{r_{cr}} = \frac{r_P}{r_{cr}} \left\{ \sin^2 \theta_P + 2\left(\cos \theta_P - \cos \theta_C\right)\left(\sqrt{M_P^2 - 1} \sin \theta_P + \cos \theta_P\right) \right\}^{1/2} \tag{11}$$

which is the same result as that given by Foelsch (equation (17) of reference 7). The x-coordinate of point K is then obtained by integration of the relation $d\frac{x}{r_{cr}} = \frac{d\frac{R}{r_{cr}}}{\tan(\theta + \mu)}$ along the left Mach line from P to K on the assumption that $\theta = \theta_P$ and $M = M_P$ as before. The result is

$$\frac{x_K}{r_{cr}} = \frac{\frac{R_K}{r_{cr}} - \frac{r_P}{r_{cr}} \sin \theta_P}{\tan\left(\theta_P + \mu_P\right)} + \frac{r_P}{r_{cr}} \cos \theta_P \tag{12}$$

since

$$\frac{x_P}{r_{cr}} = \frac{r_P}{r_{cr}} \cos \theta_P$$

and

$$\frac{R_P}{r_{cr}} = \frac{r_P}{r_{cr}} \sin \theta_P$$

An approximation which is more accurate for the Mach number 10 nozzle than that given by Foelsch (reference 7 or equations (11) and (12) herein) for the transition streamlines can be obtained from a consideration of the geometric properties of the flow in region IV (see sketch on p. 10). Thus, if PK is assumed to be a straight line, (that is, $M = M_P$ and $\theta = \theta_P$ along PK), as was done in the derivation of equations (11) and (12), the coordinates of point K are

$$\left.\begin{aligned} \frac{x_K}{r_{cr}} &= \frac{r_P}{r_{cr}} \cos \theta_P + \frac{\Delta s_K}{r_{cr}} \cos \left(\theta_P + \mu_P\right) \\ \frac{R_K}{r_{cr}} &= \frac{r_P}{r_{cr}} \sin \theta_P + \frac{\Delta s_K}{r_{cr}} \sin \left(\theta_P + \mu_P\right) \end{aligned}\right\} \tag{13}$$

where Δs_K is the length of the Mach line PK. To obtain an expression for Δs, first consider its value for the final Mach cone DE. Thus,

$$\sin \mu_D = \frac{1}{M_D} = \frac{R_E}{\Delta s_E} \tag{14}$$

If the flow were allowed to expand from point C as an undisturbed radial flow until it reached the spherical segment DD', the density and velocity would be the same at the surface of this spherical segment as it is along the final Mach cone DE. Therefore, conservation of mass requires that the surface area of the spherical segment DD' be equal to the plane cross-sectional area at E; that is,

$$R_E = 2r_D \sin \frac{\theta_C}{2}$$

Then, from equation (14),

$$\Delta s_E = 2M_D \, r_D \sin \frac{\theta_C}{2}$$

The same reasoning may be applied to obtain an approximate relation between the area of the spherical segment formed by rotation of arc PP' about the radial line OP and the area $\pi(KK')^2$, where the line KK' is

normal to the radial streamline extended through point P. Thus, assuming uniform flow along PK gives

$$\Delta s_K = 2M_P r_P \sin \frac{\theta_C - \theta_P}{2} \tag{15}$$

This relation for Δs_K can be obtained only by assuming that the line OP is, in effect, the axis of a new nozzle with a final Mach cone of half angle μ_P. This assumption is compatible with the supposition that the flow along PK is parallel and uniform. Substitution of equation (15) into equations (13) results in

$$\left.\begin{aligned} \frac{x_K}{r_{cr}} &= \frac{r_P}{r_{cr}} \left[\cos \theta_P + 2M_P \sin \frac{\theta_C - \theta_P}{2} \cos \left(\theta_P + \mu_P\right)\right] \\ \frac{R_K}{r_{cr}} &= \frac{r_P}{r_{cr}} \left[\sin \theta_P + 2M_P \sin \frac{\theta_C - \theta_P}{2} \sin \left(\theta_P + \mu_P\right)\right] \end{aligned}\right\} \tag{16}$$

In equations (16) the values of r_P, θ_P, and θ_C depend on the radial flow in region III (fig. 1). As discussed previously this flow is determined by the specification of the final expansion angle θ_{I_D} and Mach number at point D.

The transition streamline through point C has been computed for the Mach number 10 nozzle by Foelsch's method (equations (11) and (12)) and the geometric method given by equations (16). The results of the two computations are compared in table IV to the streamline coordinates obtained by the method of characteristics with the fine mesh. A comparison between the streamline coordinates from the coarse and fine mesh is also included. The maximum error from Foelsch's method is about 12 percent as compared to an error of 4 percent by the geometric method. Although both methods result in significant error for this nozzle, even in comparison with the values obtained by the characteristic method for the coarse net, the possibility is that both methods may be more accurate at lower Mach numbers where smaller values of θ_C can be used.

Cross-section contours.- The nozzle may be designed for a test section of arbitrary cross-sectional shape. Thus, the distance from the axis to a point on an arbitrary closed curve in a cross-sectional plane

of the final parallel and uniform flow region is the R ordinate of the starting point of a streamline which will be traced through the flow field to the minimum. Because of the symmetry of the flow field all streamlines bounding the nozzle can be designed in a single meridian plane. For the Mach number 10 nozzle a square cross section was specified in the uniform-flow region. Some of the resulting nozzle cross-section contours are shown in figure 4. The cross section at the minimum is square since the flow at this station is assumed to be parallel and uniform. The maximum deviation of the other contours from a square is approximately 0.3. Nondimensional coordinates for the Mach number 10 nozzle are presented in table V. The geometrical minimum is located at $x_A = 0.5043\ r_{cr}$ for reasons noted previously.

CONCLUDING REMARKS

A method is given for the design of three-dimensional nozzles utilizing axisymmetric flow. The nozzle can be designed to produce parallel and uniform flow in a test chamber of arbitrary cross section. Design calculations are made for a Mach number 10 nozzle in which a square test section is specified to reduce the possibility of axisymmetric imperfections at the wall and to provide for the installation of schlieren windows. The specification of radial flow in a portion of the flow field in general assures a physically possible solution and results in an appreciable reduction of computing time. The flow in the immediate vicinity of the axis of symmetry is computed by a simplified but sufficiently accurate method whereby the hodograph of any isentropic axisymmetric flow is determined. The remainder of the supersonic flow field is constructed by the method of characteristics. The effect of mesh size on the accuracy of the calculation is obtained by comparing streamlines through two flow fields computed with steps of different size. This comparison indicates for the Mach number 10 nozzle computation of this paper that the relative increase in accuracy is of the same order as the decrease in mesh size. Of the two methods considered for determining the final streamlines from the flow net, the stream-function method proved to be the most convenient and accurate. Foelsch's analytic expressions for the transition streamlines give coordinates which deviate from the flow net streamlines for the Mach number 10 nozzle by as much as 12 percent. Similar analytic expressions derived in this paper from the geometric properties of the flow result in transition streamline coordinates with a maximum error of about 4 percent.

Langley Aeronautical Laboratory
National Advisory Committee for Aeronautics
Langley Field, Va., April 1, 1952

APPENDIX

THREE-DIMENSIONAL RADIAL FLOW

For the steady flow of a gas in the absence of viscosity and heat transfer, there is obtained (reference 8, p. 553)

$$c^2 \nabla \cdot \bar{V} = \frac{1}{2} \bar{V} \cdot \nabla V^2 \tag{A1}$$

if the flow along each streamline is assumed adiabatic.

If the fluid moves radially and the velocity and speed of sound are functions of r only (where r is the distance from a fixed point), equation (A1) becomes

$$\left(1 - \frac{V_r^2}{c^2}\right)\frac{dV_r}{dr} + 2\frac{V_r}{r} = 0$$

or, since V_r is the only velocity component

$$\left(1 - M^2\right)\frac{dV}{dr} + 2\frac{V}{r} = 0 \tag{A2}$$

From the adiabatic energy equation the relation between Mach number and velocity is

$$\frac{dV}{V} = \frac{1}{1 + \frac{\gamma - 1}{2} M^2}\frac{dM}{M} \tag{A3}$$

Then, combining equation (A2) and (A3) gives

$$\frac{dr}{r} = \frac{1}{2}\frac{M^2 - 1}{1 + \frac{\gamma - 1}{2} M^2}\frac{dM}{M} \tag{A4}$$

Integrating equation (A4) between the limits $r = r_{cr}$ to r and $M = 1$ to M gives

$$\frac{r}{r_{cr}} = \left\{ \frac{\left[\frac{2}{\gamma + 1} \left(1 + \frac{\gamma - 1}{2} M^2 \right) \right]^{\frac{\gamma+1}{2(\gamma-1)}}}{M} \right\}^{1/2} \tag{A5}$$

The characteristic equations are now easily determined (see the following sketch):

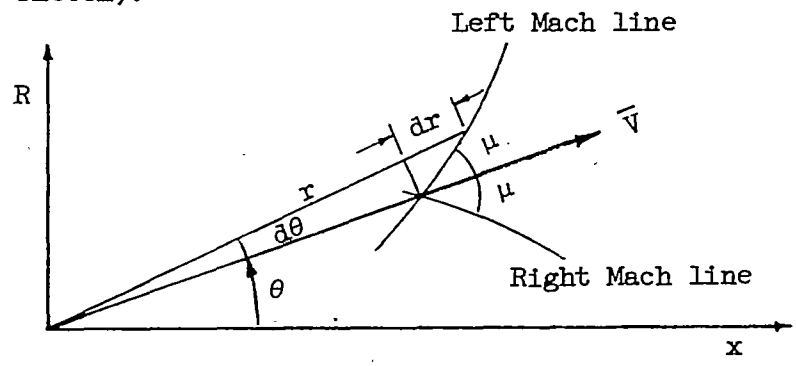

For the left Mach line

$$\frac{dR}{dx} = \tan(\theta + \mu) \tag{A6}$$

and

$$\frac{dr}{r\, d\theta} = \cot \mu \tag{A7}$$

Combining equations (A4) and (A7) gives

$$d\theta = \frac{1}{2} \frac{\sqrt{M^2 - 1}}{1 + \frac{\gamma - 1}{2} M^2} \frac{dM}{M} \tag{A8}$$

since $\cot \mu = \sqrt{M^2 - 1}$. Integration of equation (A8) from $\theta = 0$ to θ_I and $M = 1$ to M gives

$$\theta_I = \frac{1}{2}\sqrt{\frac{\gamma + 1}{\gamma - 1}} \tan^{-1}\left[\frac{\gamma - 1}{\gamma + 1}\left(M^2 - 1\right)\right]^{1/2} - \frac{1}{2}\cos^{-1}\frac{1}{M} \tag{A9}$$

Similarly, for the right Mach line,

$$\frac{dR}{dx} = \tan(\theta - \mu) \tag{A10}$$

and

$$\theta_I = -\frac{1}{2}\sqrt{\frac{\gamma + 1}{\gamma - 1}} \tan^{-1}\left[\frac{\gamma - 1}{\gamma + 1}\left(M^2 - 1\right)\right]^{1/2} + \frac{1}{2}\cos^{-1}\frac{1}{M} \tag{A11}$$

Equations (A5) and (A9) have been computed and tabulated for $\theta_I = 0^\circ$ to 53.375° in intervals of 0.125° in table I. Equation (A9) is used since the conventional definition of the total expansion angle is such that a positive increase in M results in a positive increase in θ_I regardless of whether the Mach line is of the right or left family.

The Mach lines BC and CD (fig. 1) may now be constructed as follows: The final Mach number is taken as $M_D = 10.068$ which gives $\theta_{I_D} = 51.25^\circ$ from table I. The flow variables M and r/r_{cr} for any point on line CD are tabulated with the argument $\theta_I = \theta_{I_D} - \theta$, where the local flow angle θ is the parameter. Thus, if $\theta = 4^\circ$, $\theta_I = 47.25^\circ$; then from table I, $M = 7.733272$ and $r/r_{cr} = 12.77156$. From this value of r/r_{cr} and the given value of θ the coordinates of the point can be obtained since

$$\frac{x}{r_{cr}} = \frac{r}{r_{cr}}\cos\theta = 12.7404$$

$$\frac{R}{r_{cr}} = \frac{r}{r_{cr}}\sin\theta = 0.8909$$

For this particular nozzle, the flow angle at point C was taken as 16° which gives $\theta_{I_C} = 35.25^\circ$ and $\theta_{I_B} = 19.25^\circ$ since $\theta_B = 0^\circ$.

REFERENCES

1. McLellan, Charles H., Williams, Thomas W., and Beckwith, Ivan E.: Investigation of the Flow Through a Single-Stage Two-Dimensional Nozzle in the Langley 11-Inch Hypersonic Tunnel. NACA TN 2223, 1950.

2. McLellan, Charles H., Williams, Thomas W., and Bertram, Mitchel H.: Investigation of a Two-Step Nozzle in the Langley 11-Inch Hypersonic Tunnel. NACA TN 2171, 1950.

3. Meyer, R. E.: The Method of Characteristics for Problems of Compressible Flow Involving Two Independent Variables.
Part I - The General Theory (with a Note on the Calculation of Axially-Symmetrical Supersonic Flows by S. Goldstein). Jour. Mech. and Appl. Math., vol. 1, pt. 2, June 1948, pp. 196-219.
Part II - Integration Along a Mach Line. The Radial Focusing Effect in Axially Symmetrical Flow. Jour. Mech. and Appl. Math., vol. 1, pt. 4, Dec. 1948, pp. 451-469.

4. Tsien, Hsue-Shen: On the Design of the Contraction Cone for a Wind Tunnel. Jour. Aero. Sci., vol. 10, no. 2, Feb. 1943, pp. 68-70.

5. Szczeniowski, Boleslaw: Contraction Cone for a Wind Tunnel. Jour. Aero. Sci., vol. 10, no. 8, Oct. 1943, pp. 311-312. (Errata issued, vol. 11, no. 2, Apr. 1944, p. 173.)

6. Sauer, R.: Method of Characteristics for Three-Dimensional Axially Symmetrical Supersonic Flows. NACA TM 1133, 1947.

7. Foelsch, Kuno: The Analytical Design of an Axially Symmetric Laval Nozzle for a Parallel and Uniform Jet. Jour. Aero. Sci., vol. 16, no. 3, March 1949, pp. 161-166, 188.

8. Milne-Thomson, L. M.: Theoretical Hydrodynamics, Sec. ed., Macmillan & Co., 1949.

9. Isenberg, J. S.: The Method of Characteristics in Compressible Flow. Part I (Steady Supersonic Flow). Tech. Rep. No. F-TR-1173-ND, ATI No. 26341, Air Material Command, U. S. Air Force, Dec. 1947.

10. Ferri, Antonio: Elements of Aerodynamics of Supersonic Flows. The Macmillan Co., 1949.

TABLE I.- THREE DIMENSIONAL RADIAL FLOW VARIABLES

θ_I (deg)	M	μ (deg)	r/r_{cr}	θ_I (deg)	M	μ (deg)	r/r_{cr}	θ_I (deg)	M	μ (deg)	r/r_{cr}
0.000	1.000000	90.00000	1.000000	5.000	1.434975	44.17691	1.065320	10.000	1.774976	34.29042	1.188383
0.125	1.031794	75.73956	1.000414	5.125	1.443555	43.84693	1.067728	10.125	1.783592	34.10189	1.192205
0.250	1.050876	72.09867	1.001049	5.250	1.452118	43.52328	1.070169	10.250	1.792220	33.91534	1.196065
0.375	1.067123	69.56999	1.001811	5.375	1.460666	43.20566	1.072644	10.375	1.800863	33.73064	1.199966
0.500	1.081813	67.57420	1.002671	5.500	1.469200	42.89387	1.075153	10.500	1.809519	33.54784	1.203907
0.625	1.095473	65.90190	1.003612	5.625	1.477721	42.58769	1.077694	10.625	1.818190	33.36684	1.207888
0.750	1.108387	64.45040	1.004627	5.750	1.486230	42.28691	1.080268	10.750	1.826878	33.18759	1.211912
0.875	1.120724	63.16122	1.005705	5.875	1.494728	41.99135	1.082876	10.875	1.835579	33.01014	1.215973
1.000	1.132602	61.99698	1.006845	6.000	1.503217	41.70074	1.085517	11.000	1.844297	32.83436	1.220077
1.125	1.144102	60.93252	1.008041	6.125	1.511699	41.41494	1.088192	11.125	1.853030	32.66028	1.224223
1.250	1.155284	59.94993	1.009289	6.250	1.520173	41.13383	1.090900	11.250	1.861781	32.48781	1.228412
1.375	1.166194	59.03596	1.010588	6.375	1.528641	40.85718	1.093643	11.375	1.870548	32.31698	1.232641
1.500	1.176870	58.18034	1.011934	6.500	1.537103	40.58493	1.096417	11.500	1.879333	32.14771	1.236913
1.625	1.187341	57.37511	1.013328	6.625	1.545562	40.31684	1.099226	11.625	1.888135	31.98001	1.241228
1.750	1.197627	56.61424	1.014764	6.750	1.554018	40.05279	1.102070	11.750	1.896957	31.81379	1.245587
1.875	1.207754	55.89213	1.016245	6.875	1.562470	39.79273	1.104947	11.875	1.905796	31.64907	1.249990
2.000	1.217735	55.20479	1.017768	7.000	1.570921	39.53647	1.107858	12.000	1.914655	31.48582	1.254437
2.125	1.227586	54.54851	1.019330	7.125	1.579370	39.28395	1.110803	12.125	1.923532	31.32401	1.258927
2.250	1.237319	53.92035	1.020934	7.250	1.587820	39.03495	1.113783	12.250	1.932430	31.16359	1.263462
2.375	1.246947	53.31758	1.022576	7.375	1.596270	38.78948	1.116797	12.375	1.941347	31.00456	1.268043
2.500	1.256475	52.73821	1.024257	7.500	1.604721	38.54737	1.119846	12.500	1.950286	30.84687	1.272669
2.625	1.265912	52.18032	1.025977	7.625	1.613175	38.30851	1.122930	12.625	1.959245	30.69054	1.277341
2.750	1.275269	51.64199	1.027731	7.750	1.621632	38.07284	1.126049	12.750	1.968225	30.53550	1.282060
2.875	1.284550	51.12189	1.029525	7.875	1.630091	37.84031	1.129202	12.875	1.977226	30.38175	1.286824
3.000	1.293762	50.61863	1.031353	8.000	1.638554	37.61078	1.132392	13.000	1.986250	30.22926	1.291637
3.125	1.302911	50.13102	1.033218	8.125	1.647022	37.38419	1.135616	13.125	1.995297	30.07800	1.296497
3.250	1.312000	49.65810	1.035119	8.250	1.655496	37.16042	1.138876	13.250	2.004364	29.92801	1.301404
3.375	1.321034	49.19895	1.037054	8.375	1.663975	36.93945	1.142172	13.375	2.013457	29.77916	1.306361
3.500	1.330016	48.75268	1.039024	8.500	1.672461	36.72117	1.145505	13.500	2.022571	29.63153	1.311366
3.625	1.338953	48.31844	1.041029	8.625	1.680952	36.50558	1.148872	13.625	2.031711	29.48502	1.316421
3.750	1.347846	47.89562	1.043070	8.750	1.689452	36.29251	1.152278	13.750	2.040873	29.33969	1.321524
3.875	1.356699	47.48353	1.045143	8.875	1.697961	36.08195	1.155719	13.875	2.050060	29.19546	1.326679
4.000	1.365514	47.08167	1.047251	9.000	1.706477	35.87385	1.159198	14.000	2.059273	29.05233	1.331885
4.125	1.374296	46.68935	1.049392	9.125	1.715002	35.66815	1.162713	14.125	2.068510	28.91030	1.337142
4.250	1.383042	46.30637	1.051566	9.250	1.723537	35.46479	1.166266	14.250	2.077771	28.76936	1.342448
4.375	1.391761	45.93195	1.053776	9.375	1.732082	35.26366	1.169857	14.375	2.087061	28.62942	1.347810
4.500	1.400450	45.56592	1.056017	9.500	1.740638	35.06476	1.173485	14.500	2.096376	28.49054	1.353222
4.625	1.409116	45.20786	1.058292	9.625	1.749204	34.86808	1.177152	14.625	2.105717	28.35269	1.358689
4.750	1.417757	44.85700	1.060602	9.750	1.757783	34.67345	1.180856	14.750	2.115087	28.21579	1.364210
4.875	1.426375	44.51355	1.062944	9.875	1.766373	34.48094	1.184600	14.875	2.124481	28.07995	1.369783

TABLE I.- THREE DIMENSIONAL RADIAL FLOW VARIABLES - Continued

θ_I (deg)	M	μ (deg)	r/r_{cr}	θ_I (deg)	M	μ (deg)	r/r_{cr}	θ_I (deg)	M	μ (deg)	r/r_{cr}
15.000	2.133906	27.94504	1.375413	20.000	2.537816	23.20610	1.652765	25.000	3.012611	19.38644	2.070200
15.125	2.143357	27.81109	1.381097	20.125	2.548698	23.10125	1.661216	25.125	3.025662	19.29950	2.083103
15.250	2.152837	27.67809	1.386836	20.250	2.559626	22.99695	1.669756	25.250	3.038785	19.21288	2.096155
15.375	2.162346	27.54600	1.392633	20.375	2.570603	22.89316	1.678386	25.375	3.051969	19.12665	2.109347
15.500	2.171884	27.41485	1.398487	20.500	2.581621	22.78994	1.687100	25.500	3.065224	19.04074	2.122690
15.625	2.181451	27.28459	1.404398	20.625	2.592683	22.68726	1.695904	25.625	3.078551	18.95516	2.136186
15.750	2.191048	27.15522	1.410367	20.750	2.603797	22.58506	1.704803	25.750	3.091947	18.86992	2.149836
15.875	2.200676	27.02672	1.416396	20.875	2.614952	22.48343	1.713789	25.875	3.105408	18.78506	2.163634
16.000	2.210333	26.89910	1.422482	21.000	2.626156	22.38231	1.722869	26.000	3.118939	18.70053	2.177588
16.125	2.220022	26.77230	1.428629	21.125	2.637408	22.28168	1.732044	26.125	3.132548	18.61630	2.191706
16.250	2.229743	26.64635	1.434839	21.250	2.648706	22.18156	1.741313	26.250	3.146220	18.53245	2.205978
16.375	2.239494	26.52124	1.441107	21.375	2.660056	22.08193	1.750679	26.375	3.159972	18.44888	2.220420
16.500	2.249279	26.39691	1.447438	21.500	2.671453	21.98280	1.760143	26.500	3.173790	18.36569	2.235018
16.625	2.259095	26.27342	1.453832	21.625	2.682899	21.88415	1.769705	26.625	3.187689	18.28277	2.249792
16.750	2.268944	26.15071	1.460288	21.750	2.694397	21.78598	1.779370	26.750	3.201665	18.20015	2.264739
16.875	2.278827	26.02877	1.466809	21.875	2.705941	21.68831	1.789130	26.875	3.215705	18.11793	2.279845
17.000	2.288742	25.90762	1.473394	22.000	2.717541	21.59107	1.798997	27.000	3.229833	18.03594	2.295138
17.125	2.298691	25.78721	1.480044	22.125	2.729191	21.49432	1.808968	27.125	3.244036	17.95428	2.310607
17.250	2.308676	25.66756	1.486761	22.250	2.740889	21.39805	1.819039	27.250	3.258316	17.87293	2.326253
17.375	2.318696	25.54862	1.493544	22.375	2.752648	21.30217	1.829225	27.375	3.272676	17.79188	2.342086
17.500	2.328750	25.43045	1.500394	22.500	2.764456	21.20677	1.839514	27.500	3.287112	17.71115	2.358100
17.625	2.338840	25.31297	1.507313	22.625	2.776313	21.11186	1.849909	27.625	3.301632	17.63039	2.374302
17.750	2.348965	25.19621	1.514300	22.750	2.788231	21.01733	1.860419	27.750	3.316232	17.55055	2.390696
17.875	2.359126	25.08017	1.521357	22.875	2.800196	20.92330	1.871036	27.875	3.330917	17.47067	2.407288
18.000	2.369324	24.96479	1.528484	23.000	2.812223	20.82965	1.881772	28.000	3.345682	17.39111	2.424071
18.125	2.379561	24.85010	1.535683	23.125	2.824301	20.73645	1.892616	28.125	3.360533	17.31182	2.441056
18.250	2.389834	24.73609	1.542953	23.250	2.836437	20.64367	1.903581	28.250	3.375468	17.23282	2.458243
18.375	2.400144	24.62274	1.550296	23.375	2.848633	20.55128	1.914666	28.375	3.390490	17.15410	2.475637
18.500	2.410491	24.51009	1.557711	23.500	2.860885	20.45931	1.925867	28.500	3.405600	17.07565	2.493241
18.625	2.420880	24.39803	1.565203	23.625	2.873194	20.36777	1.937190	28.625	3.420797	16.99747	2.511055
18.750	2.431306	24.28663	1.572769	23.750	2.885562	20.27661	1.948635	28.750	3.436083	16.91957	2.529088
18.875	2.441773	24.17585	1.580412	23.875	2.897990	20.18587	1.960204	28.875	3.451456	16.84195	2.547332
19.000	2.452279	24.06570	1.588131	24.000	2.910476	20.09552	1.971899	29.000	3.466924	16.76460	2.565804
19.125	2.462826	23.95617	1.595929	24.125	2.923024	20.00557	1.983722	29.125	3.482485	16.68749	2.584502
19.250	2.473411	23.84727	1.603803	24.250	2.935635	19.91597	1.995674	29.250	3.498132	16.61067	2.603424
19.375	2.484040	23.73895	1.611759	24.375	2.948304	19.82680	2.007756	29.375	3.513871	16.53413	2.622574
19.500	2.494711	23.63121	1.619795	24.500	2.961040	19.73797	2.019973	29.500	3.529710	16.45782	2.641965
19.625	2.505423	23.52407	1.627913	24.625	2.973836	19.64954	2.032323	29.625	3.545650	16.38175	2.661603
19.750	2.516177	23.41751	1.636112	24.750	2.986696	19.56147	2.044809	29.750	3.561680	16.30596	2.681476
19.875	2.526976	23.31151	1.644397	24.875	2.999617	19.47380	2.057430	29.875	3.577807	16.23042	2.701595

NACA

TABLE I.- THREE DIMENSIONAL RADIAL FLOW VARIABLES - Continued

θ_I (deg)	M	μ (deg)	r/r_{cr}	θ_I (deg)	M	μ (deg)	r/r_{cr}	θ_I (deg)	M	μ (deg)	r/r_{cr}
30.000	3.594036	16.15513	2.721968	35.000	4.338993	13.32464	3.799083	40.000	5.347855	10.77723	5.730382
30.125	3.610367	16.08006	2.742601	35.125	4.360440	13.25791	3.834330	40.125	5.377847	10.71641	5.796840
30.250	3.626798	16.00525	2.763488	35.250	4.382051	13.19134	3.870090	40.250	5.408108	10.65575	5.864029
30.375	3.643330	15.93069	2.784639	35.375	4.403829	13.12494	3.906381	40.375	5.438667	10.59518	5.932632
30.500	3.659967	15.85636	2.806060	35.500	4.425770	13.05872	3.943199	40.500	5.469510	10.53474	6.002430
30.625	3.676706	15.78227	2.827748	35.625	4.447883	12.99265	3.980564	40.625	5.500654	10.47443	6.073478
30.750	3.693553	15.70844	2.849714	35.750	4.470164	12.92677	4.018480	40.750	5.532091	10.41423	6.145782
30.875	3.710504	15.63483	2.871958	35.875	4.492622	12.86105	4.056964	40.875	5.563835	10.35416	6.219390
31.000	3.727567	15.56144	2.894492	36.000	4.515247	12.79550	4.096013	41.000	5.595886	10.29421	6.294318
31.125	3.744736	15.48830	2.917311	36.125	4.538057	12.73010	4.135655	41.125	5.628254	10.23437	6.370613
31.250	3.762019	15.41537	2.940428	36.250	4.561041	12.66488	4.175889	41.250	5.660938	10.17464	6.448293
31.375	3.779413	15.34268	2.963843	36.375	4.584213	12.59981	4.216740	41.375	5.693947	10.11504	6.527397
31.500	3.796917	15.27021	2.987560	36.500	4.607576	12.53488	4.258224	41.500	5.727284	10.05555	6.607954
31.625	3.814543	15.19795	3.011595	36.625	4.631111	12.47016	4.300310	41.625	5.760956	9.996165	6.690007
31.750	3.832278	15.12593	3.035935	36.750	4.654848	12.40555	4.343067	41.750	5.794963	9.936909	6.773579
31.875	3.850136	15.05411	3.060605	36.875	4.678775	12.34110	4.386479	41.875	5.829316	9.877761	6.858712
32.000	3.868107	14.98253	3.085589	37.000	4.702891	12.27683	4.430548	42.000	5.864022	9.818721	6.945452
32.125	3.886204	14.91114	3.110914	37.125	4.727211	12.21269	4.475317	42.125	5.899085	9.759789	7.033836
32.250	3.904420	14.83997	3.136573	37.250	4.751728	12.14871	4.520779	42.250	5.934508	9.700965	7.123901
32.375	3.922754	14.76902	3.162565	37.375	4.776447	12.08489	4.566951	42.375	5.970300	9.642249	7.215683
32.500	3.941220	14.69826	3.188917	37.500	4.801372	12.02122	4.613849	42.500	6.006466	9.583641	7.309230
32.625	3.959808	14.62773	3.215618	37.625	4.826509	11.95768	4.661499	42.625	6.043009	9.525150	7.404582
32.750	3.978517	14.55741	3.242669	37.750	4.851853	11.89430	4.709894	42.750	6.079943	9.466749	7.501795
32.875	3.997367	14.48726	3.270104	37.875	4.877414	11.83107	4.759069	42.875	6.117267	9.408465	7.600902
33.000	4.016340	14.41734	3.297901	38.000	4.903193	11.76798	4.809031	43.000	6.154993	9.350280	7.701961
33.125	4.035444	14.34762	3.326075	38.125	4.929189	11.70503	4.859793	43.125	6.193125	9.292194	7.805020
33.250	4.054684	14.27809	3.354639	38.250	4.955408	11.64223	4.911379	43.250	6.231668	9.234216	7.910119
33.375	4.074059	14.20875	3.383597	38.375	4.981859	11.57955	4.963810	43.375	6.270631	9.176346	8.017317
33.500	4.093568	14.13962	3.412947	38.500	5.008540	11.51702	5.017099	43.500	6.310028	9.118566	8.126689
33.625	4.113218	14.07068	3.442708	38.625	5.035449	11.45464	5.071254	43.375	6.349856	9.060885	8.238264
33.750	4.133011	14.00192	3.472889	38.750	5.062600	11.39239	5.126313	43.750	6.390127	9.003312	8.352106
33.875	4.152937	13.93338	3.503477	38.875	5.089987	11.33027	5.182276	43.875	6.430852	8.945819	8.468292
34.000	4.173019	13.86499	3.534514	39.000	5.117620	11.26829	5.239174	44.000	6.472035	8.888435	8.586866
34.125	4.193232	13.79683	3.565961	39.125	5.145493	11.20646	5.297011	44.125	6.513685	8.831145	8.707892
34.250	4.213603	13.72881	3.597873	39.250	5.173622	11.14475	5.355831	44.250	6.555806	8.773954	8.831434
34.375	4.234119	13.66100	3.630229	39.375	5.202003	11.08317	5.415645	44.375	6.598416	8.716852	8.957580
34.500	4.254785	13.59337	3.663047	39.500	5.230640	11.02173	5.476462	44.500	6.641514	8.659850	9.086375
34.625	4.275601	13.52593	3.696325	39.625	5.259543	10.96041	5.538332	44.625	6.685122	8.602932	9.217926
34.750	4.296577	13.45865	3.730094	39.750	5.288713	10.89921	5.601266	44.750	6.729234	8.546114	9.352261
34.875	4.317708	13.39155	3.764344	39.875	5.318148	10.83815	5.665272	44.875	6.773869	8.489387	9.489493

TABLE I.- THREE DIMENSIONAL RADIAL FLOW VARIABLES - Concluded

θ_I (deg)	M	μ (deg)	r/r_{cr}	θ_I (deg)	M	μ (deg)	r/r_{cr}
45.000	6.819035	8.432743	9.629704	50.000	9.210488	6.232995	19.08914
45.125	6.864735	8.376200	9.772935	50.125	9.289984	6.179450	19.47596
45.250	6.910986	8.319742	9.919312	50.250	9.370792	6.125954	19.87419
45.375	6.957808	8.263363	10.06894	50.375	9.452923	6.072529	20.28413
45.500	7.005196	8.207080	10.22187	50.500	9.536420	6.019167	20.70630
45.625	7.053160	8.150888	10.37820	50.625	9.621322	5.965855	21.14118
45.750	7.101723	8.094776	10.53806	50.750	9.707643	5.912613	21.58918
45.875	7.150888	8.038753	10.70153	50.875	9.795449	5.859429	22.05086
46.000	7.200674	7.982807	10.86872	51.000	9.884768	5.806302	22.52685
46.125	7.251085	7.926951	11.03975	51.125	9.975641	5.753228	23.01763
46.250	7.302141	7.871170	11.21471	51.250	10.06812	5.700209	23.52390
46.375	7.353850	7.815480	11.39374	51.375	10.16224	5.647240	24.04625
46.500	7.406225	7.759867	11.57695	51.500	10.25803	5.594339	24.58520
46.625	7.459280	7.704339	11.76447	51.625	10.35555	5.541491	25.14160
46.750	7.513033	7.648888	11.95645	51.750	10.45487	5.488681	25.71625
46.875	7.567491	7.593516	12.15298	51.875	10.55600	5.435939	26.30969
47.000	7.622676	7.538222	12.35426	52.000	10.65900	5.383260	26.92278
47.125	7.678598	7.483002	12.56039	52.125	10.76395	5.330615	27.55657
47.250	7.735272	7.427871	12.77156	52.250	10.87090	5.278027	28.21186
47.375	7.792717	7.372811	12.98789	52.375	10.97987	5.225494	28.88940
47.500	7.850954	7.317815	13.20961	52.500	11.09093	5.173029	29.59022
47.625	7.909983	7.262913	13.43678	52.625	11.20421	5.120585	30.31582
47.750	7.969838	7.208077	13.66967	52.750	11.31971	5.068200	31.06689
47.875	8.030530	7.153312	13.90845	52.875	11.43751	5.015865	31.84467
48.000	8.092076	7.098624	14.15330	53.000	11.55767	4.963584	32.65033
48.125	8.154501	7.044008	14.40443	53.125	11.68032	4.911338	33.48553
48.250	8.217815	6.989463	14.66202	53.250	11.80548	4.859141	34.35133
48.375	8.282047	6.934991	14.92632	53.375	11.93322	4.307005	35.24910
48.500	8.347216	6.880585	15.19756				
48.625	8.413338	6.826251	15.47595				
48.750	8.480434	6.771990	15.76173				
48.875	8.548533	6.717789	16.05518				
49.000	8.617654	6.663662	16.35656				
49.125	8.687825	6.609602	16.66616				
49.250	8.759061	6.555609	16.98423				
49.375	8.831398	6.501678	17.31112				
49.500	8.904859	6.447815	17.64712				
49.625	8.979468	6.394013	17.99257				
49.750	9.055256	6.340280	18.34780				
49.875	9.132257	6.286604	18.71322				

TABLE II.- COMPARISON OF FLOW PARAMETERS NEAR AXIS IN MACH NUMBER 10 NOZZLE AS COMPUTED BY EQUATIONS (3) AND (4)

Point (fig. 2)	Method	x/r_{cr}	R/r_{cr}	M	θ (deg)
7,6	Eq. (3)	0.55477	0.13186	1.08526	0.5889
	Eq. (4)	.55436	.12730	1.09874	.59375
	Difference	.00041	.00456	-.01348	-.00485
6,5	Eq. (3)	.67197	.08208	1.23156	1.0034
	Eq. (4)	.67194	.08153	1.23732	1.0000
	Difference	.00003	.00055	-.00576	.0034
5,4	Eq. (3)	.82688	.09904	1.44344	2.0000
	Eq. (4)	.82686	.09849	1.45212	2.0000
	Difference	.00002	.00055	-.00868	0
4,3	Eq. (3)	1.0352	.07293	1.71835	2.0000
	Eq. (4)	1.0352	.07277	1.72354	2.0000
	Difference	0	.00016	-.00519	0
3,2	Eq. (3)	1.2464	.06243	2.00013	2.0000
	Eq. (4)	1.2464	.06234	2.00436	2.0000
	Difference	0	.00009	-.00423	0
2,1	Eq. (3)	1.4737	.05731	2.30450	2.0000
	Eq. (4)	1.4737	.05724	2.30868	2.0000
	Difference	0	.00007	-.00418	0

TABLE III.- COMPARISON OF ACCURACY OF THE FLOW NETS IN MACH NUMBER 10 NOZZLE FOR $\phi = 45^{\circ}$

Point	Method	x/r_{cr}	R/r_{cr}	$\Delta R/r_{cr}$	Error (percent)
Transition streamline					
C	Exact	3.7202	1.0667		
	Desk computer	3.7202	1.0507	-0.0160	-1.50
	Bell computer	3.7202	1.0621	-.0046	-.43
Throat streamline					
A'	Exact	0.50434	0.27835		
	Desk computer	.50434	.28103	0.00268	0.96
	Bell computer	.50434	.27946	.00111	.40

TABLE IV.- COMPARISON OF STREAMLINE COORDINATES IN MACH NUMBER 10 NOZZLE FOR $\phi = 45^{\circ}$

x/r_{cr}	R/r_{cr}						
	Characteristics method			Geometric method (eq. 16)		Foelsch method	
	Fine net	Coarse net		Value	Error (percent)	Value	Error (percent)
		Value	Error (percent)				
3.7202	1.067	1.067	0	1.067	0	1.067	0
7.5	2.016	2.007	-.45	1.975	-2.03	1.919	-4.81
14.5	3.280	3.264	-.49	3.151	-3.93	2.956	-9.88
26.0	4.624	4.601	-.50	4.431	-4.17	4.067	-12.05
42.0	5.706	5.674	-.56	5.523	-3.21	5.069	-11.16
57.0	6.242	6.197	-.72	6.121	-1.94	5.704	-8.62
73.5	6.498	6.469	-.45	6.457	-.63	6.203	-4.54
89.1219	6.548	6.548	0	6.548	0	6.548	0

TABLE V.- DIMENSIONLESS COORDINATES FOR THE MACH NUMBER 10 NOZZLE

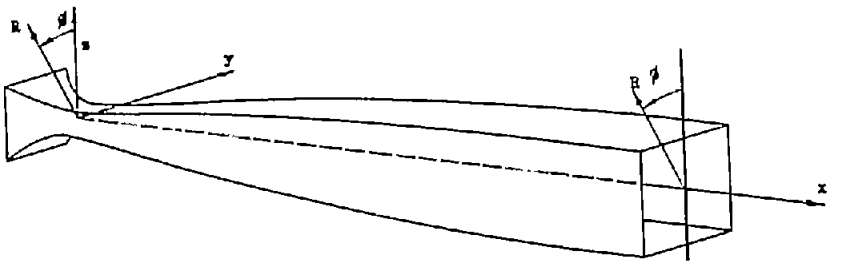

x/r_{cr}	R/r_{cr} for ϕ = —					y/r_{cr} for ϕ = —					z/r_{cr} for ϕ = —				
	45.00°	36.87°	26.57°	14.04°	0°	45.00°	36.87°	26.57°	14.04°	0°	45.00°	36.87°	26.57°	14.04°	0°
-1.9182	2.5351	2.2408	2.0042	1.8478	1.7926	1.7926	1.3445	.8963	.4482	0	1.7926	1.7926	1.7926	1.7926	1.7926
-1.4911	1.4049	1.2418	1.1107	1.0240	.9934	.9934	.7451	.4967	.2484	0	.9934	.9934	.9934	.9934	.9934
-.9614	.8432	.7452	.6666	.6145	.5962	.5962	.4471	.2981	.1490	0	.5962	.5962	.5962	.5962	.5962
-.5026	.4770	.4216	.3771	.3477	.3373	.3373	.2530	.1686	.0843	0	.3373	.3373	.3373	.3373	.3373
.0059	.2967	.2622	.2346	.2163	.2098	.2098	.1573	.1049	.0525	0	.2098	.2098	.2098	.2098	.2098
.5043	.2783	.2460	.2200	.2029	.1968	.1968	.1476	.0984	.0492	0	.1968	.1968	.1968	.1968	.1968
1.0000	.3279	.2870	.2558	.2350	.2276	.2319	.1722	.1144	.0570	0	.2319	.2296	.2288	.2280	.2276
1.5500	.4544	.3972	.3527	.3236	.3134	.3213	.2383	.1577	.0785	0	.3213	.3178	.3155	.3139	.3134
2.0500	.5905	.5172	.4602	.4228	.4096	.4175	.3103	.2058	.1025	0	.4175	.4138	.4116	.4102	.4096
2.4000	.6891	.6044	.5380	.4945	.4792	.4873	.3626	.2406	.1199	0	.4873	.4835	.4812	.4797	.4792
2.9882	.8569	.7523	.6698	.6158	.5968	.6059	.4514	.2995	.1494	0	.6059	.6018	.5991	.5974	.5968
3.7202	1.0667	.9367	.8338	.7666	.7430	.7543	.5620	.3729	.1859	0	.7543	.7494	.7458	.7437	.7430
4.9448	1.4025	1.2422	1.1083	1.0190	.9876	.9917	.7453	.4956	.2471	0	.9917	.9858	.9913	.9886	.9876
5.5962	1.5694	1.3967	1.2516	1.1550	1.1177	1.1097	.8380	.5597	.2796	0	1.1097	1.1174	1.1195	1.1186	1.1177
7.5000	2.0161	1.8131	1.6396	1.5223	1.4789	1.4256	1.0879	.7333	.3692	0	1.4256	1.4505	1.4665	1.4768	1.4789
8.5000	2.2293	2.0124	1.8261	1.7011	1.6539	1.5764	1.2074	.8167	.4126	0	1.5764	1.6099	1.6333	1.6503	1.6539
9.5000	2.4258	2.1996	2.0015	1.8697	1.8191	1.7181	1.3198	.8951	.4535	0	1.7181	1.7597	1.7902	1.8139	1.8191
11.0000	2.7068	2.4604	2.2463	2.1048	2.0496	1.9154	1.4762	1.0046	.5105	0	1.9154	1.9683	2.0092	2.0420	2.0496
14.5000	3.2801	2.9919	2.7441	2.5805	2.5179	2.3194	1.7951	1.2272	.6259	0	2.3194	2.3935	2.4544	2.5035	2.5179
17.5000	3.6975	3.3790	3.1046	2.9226	2.8552	2.6145	2.0274	1.3884	.7088	0	2.6145	2.7052	2.7768	2.8555	2.8552
21.5000	4.1737	3.8178	3.5109	3.3056	3.2318	2.9515	2.2907	1.5701	.8017	0	2.9515	3.0642	3.1402	3.2069	3.2318
26.0000	4.6235	4.2262	3.8862	3.6562	3.5750	3.2693	2.5357	1.7380	.8868	0	3.2693	3.3810	3.4758	3.5470	3.5750
30.0000	4.9602	4.5289	4.1600	3.9098	3.8225	3.5074	2.7173	1.8604	.9483	0	3.5074	3.6231	3.7208	3.7931	3.8225
34.0000	5.2484	4.7842	4.3873	4.1182	4.0237	3.7112	2.8705	1.9621	.9988	0	3.7112	3.8274	3.9241	3.9952	4.0237
38.0000	5.4956	4.9988	4.5756	4.2878	4.1866	3.8860	2.9993	2.0465	1.0399	0	3.8860	3.9990	4.0925	4.1598	4.1866
42.0000	5.7063	5.1782	4.7302	4.4240	4.3163	4.0350	3.1069	2.1154	1.0730	0	4.0350	4.1426	4.2308	4.2919	4.3163
45.0000	5.8434	5.2925	4.8262	4.5073	4.3955	4.1319	3.1755	2.1583	1.0932	0	4.1319	4.2340	4.3167	4.3727	4.3955
48.0000	5.9642	5.3912	4.9079	4.5767	4.4607	4.2173	3.2347	2.1949	1.1100	0	4.2173	4.3130	4.3898	4.4401	4.4607
53.0000	6.1350	5.5249	5.0146	4.6645	4.5417	4.3367	3.3149	2.2426	1.1313	0	4.3367	4.4199	4.4852	4.5252	4.5417
57.0000	6.2420	5.6077	5.0767	4.7128	4.5850	4.4138	3.3646	2.2704	1.1430	0	4.4138	4.4862	4.5407	4.5721	4.5850
61.0000	6.3305	5.6718	5.1218	4.7449	4.6124	4.4763	3.4051	2.2905	1.1508	0	4.4763	4.5374	4.5811	4.6032	4.6124
65.0000	6.4005	5.7194	5.1516	4.7638	4.6265	4.5258	3.4316	2.3036	1.1554	0	4.5258	4.5755	4.6077	4.6216	4.6265
67.0000	6.4294	5.7375	5.1618	4.7691	4.6292	4.5463	3.4425	2.3084	1.1567	0	4.5463	4.5906	4.6169	4.6267	4.6292
70.5000	6.4711	5.7614	5.1728	4.7724	4.6300	4.5758	3.4568	2.3133	1.1575	0	4.5758	4.6091	4.6267	4.6299	4.6300
73.5000	6.4981	5.7751	5.1762	4.7725	4.6300	4.5949	3.4651	2.3149	1.1575	0	4.5949	4.6201	4.6297	4.6300	4.6300
77.0000	6.5207	5.7846	5.1765	4.7725	4.6300	4.6108	3.4708	2.3150	1.1575	0	4.6108	4.6277	4.6300	4.6300	4.6300
80.0000	6.5338	5.7873	5.1765	4.7725	4.6300	4.6201	3.4724	2.3150	1.1575	0	4.6201	4.6298	4.6300	4.6300	4.6300
83.0000	6.5420	5.7875	5.1765	4.7725	4.6300	4.6259	3.4725	2.3150	1.1575	0	4.6259	4.6300	4.6300	4.6300	4.6300
89.1219	6.5478	5.7875	5.1765	4.7725	4.6300	4.6300	3.4725	2.3150	1.1575	0	4.6300	4.6300	4.6300	4.6300	4.6300

NACA

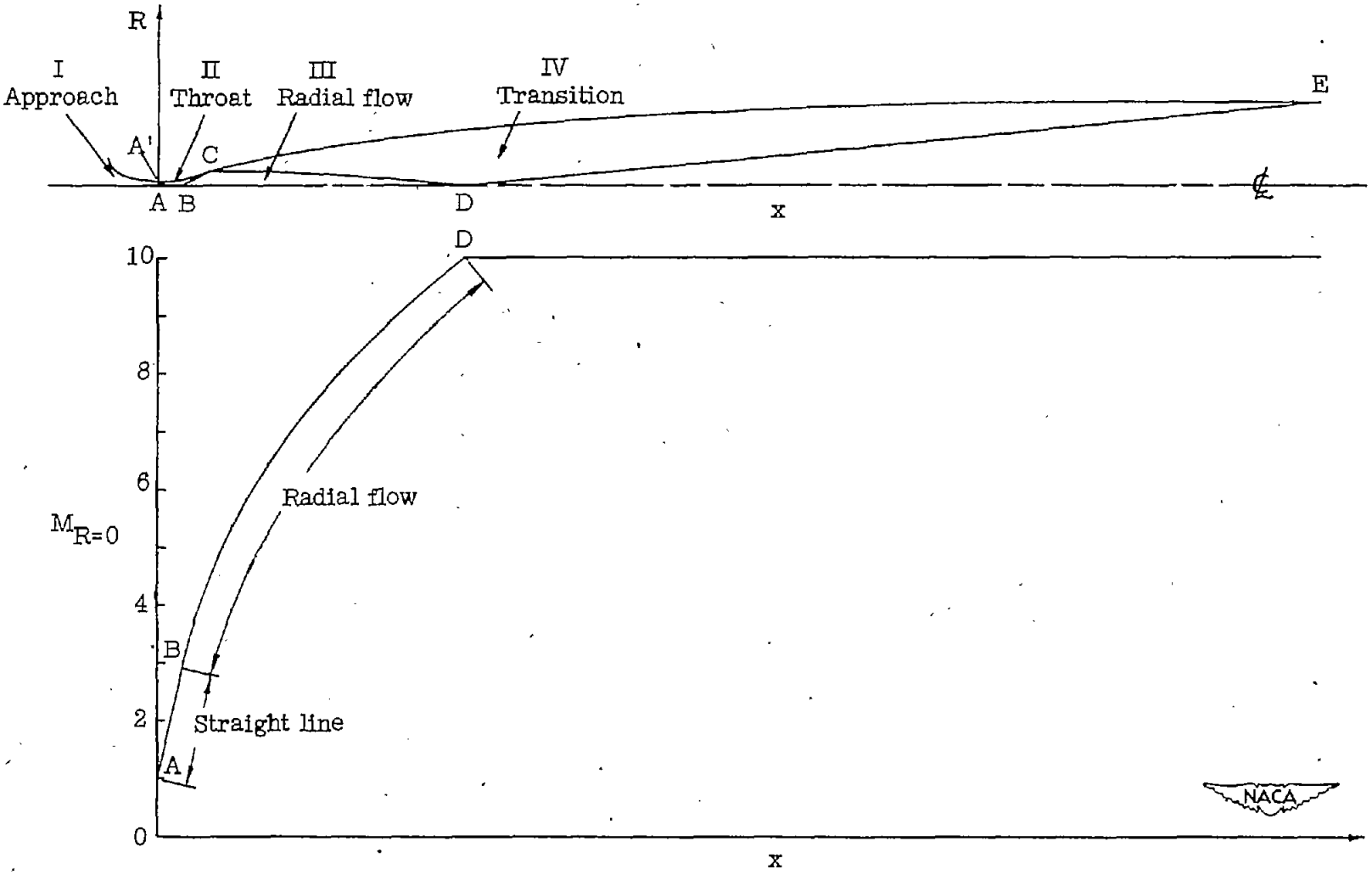

Figure 1.- Schematic representation of the nozzle flow fields showing the Mach number variation with distance along the center line for the Mach number 10 nozzle.

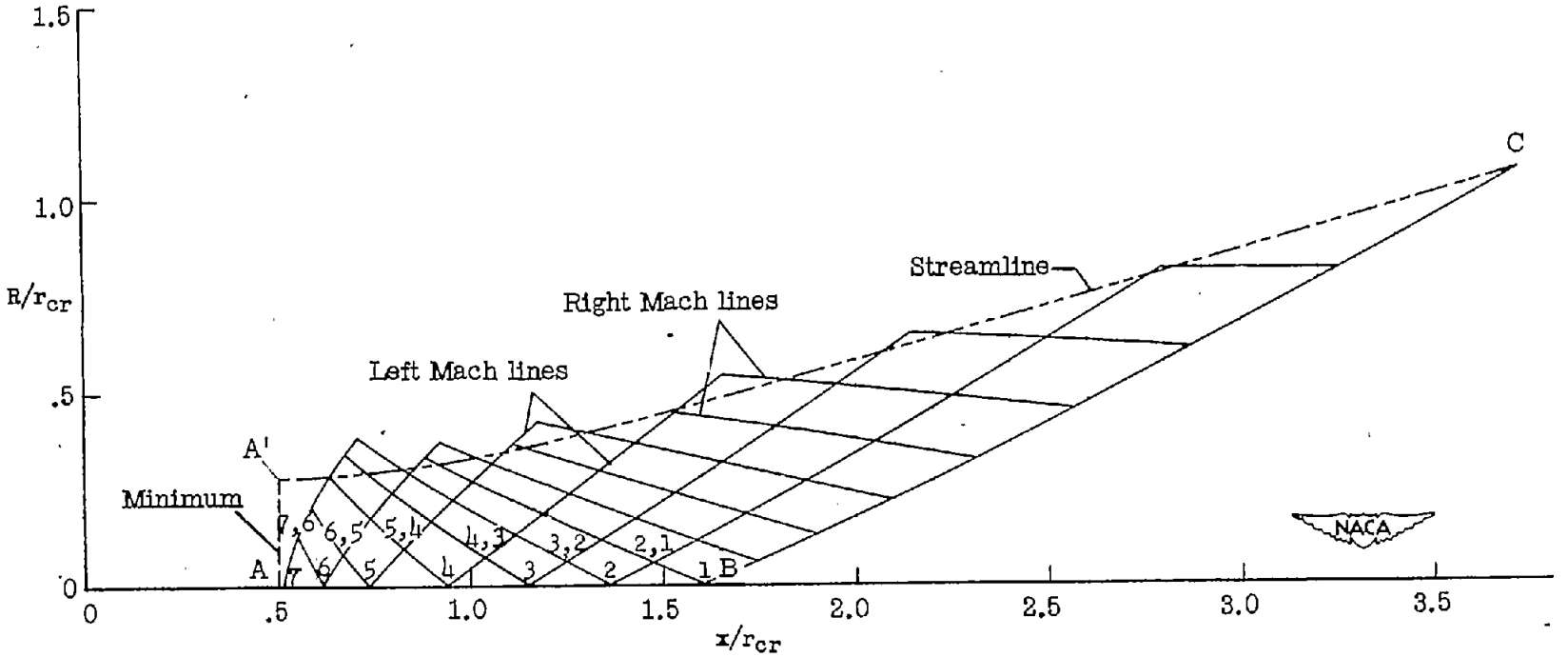

Figure 2.- Mach net in region II for the Mach number 10 nozzle with a streamline included.

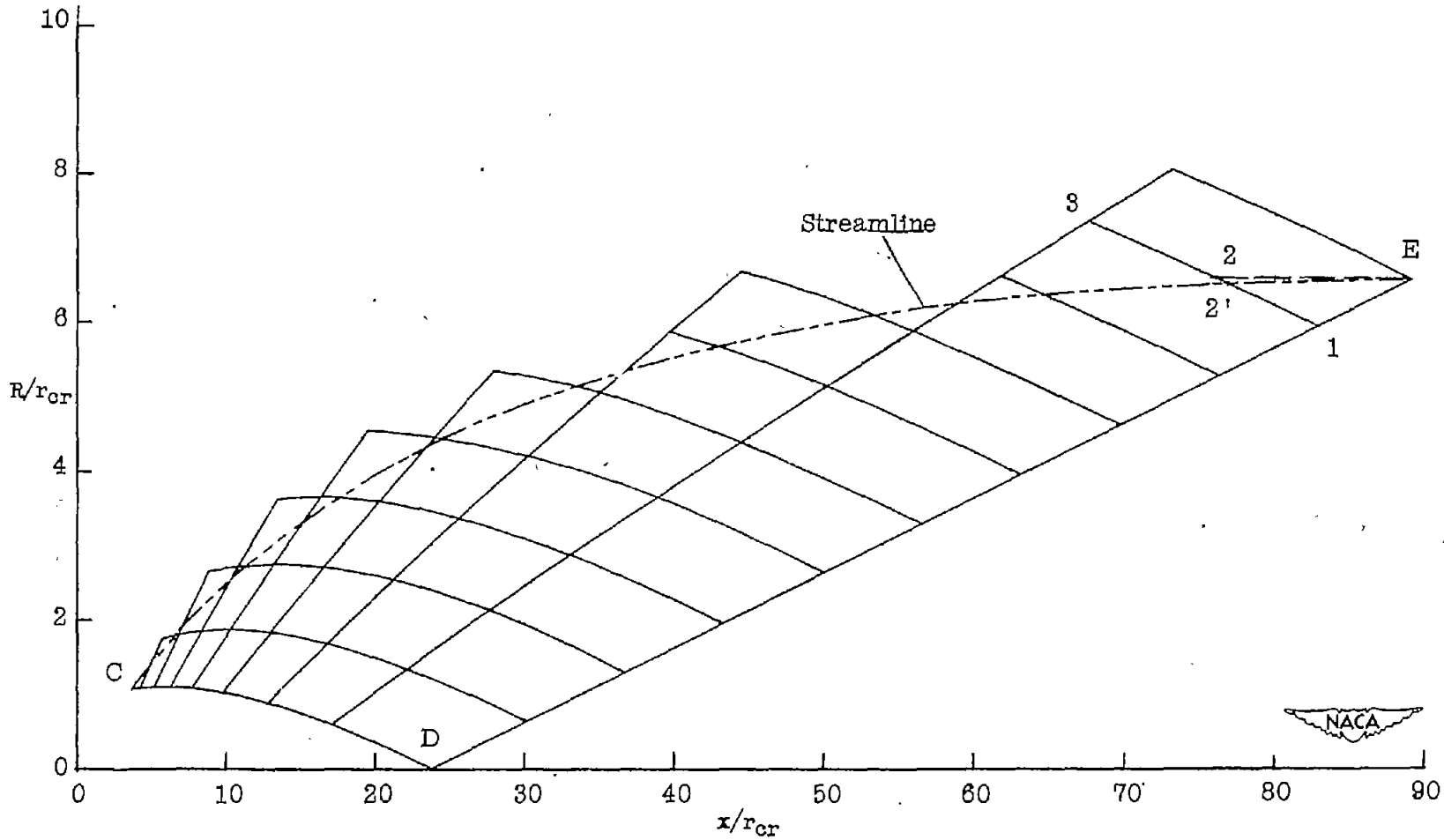

Figure 3.- Mach net in region IV for the Mach number 10 nozzle with a streamline included.

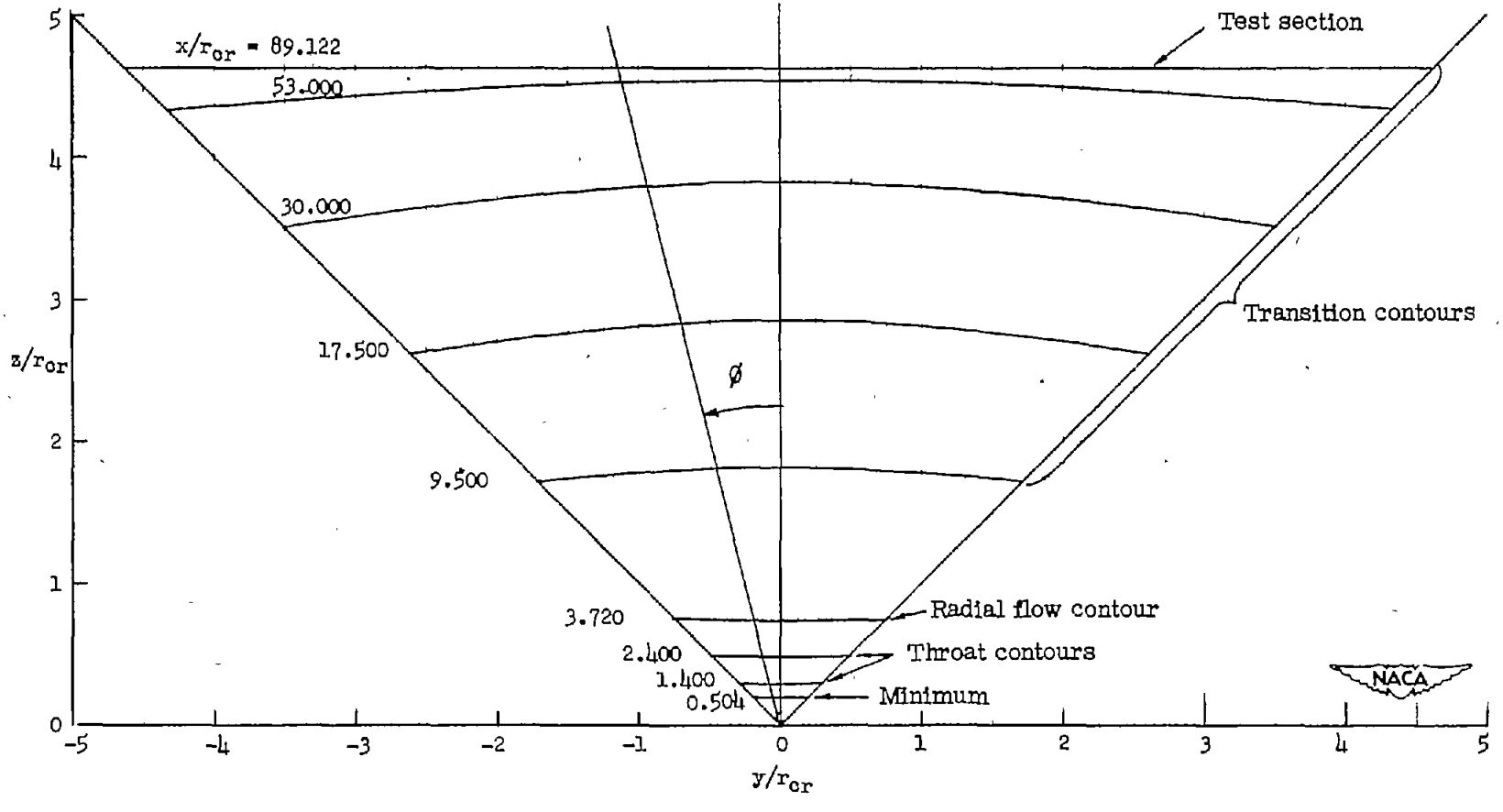

Figure 4.- Typical cross-sectional contours for one quadrant of the Mach number 10 nozzle.